

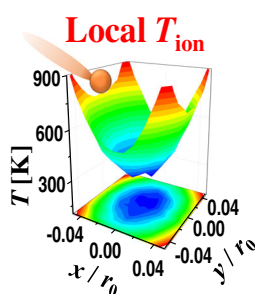
# Study of In-Trap Ion Clouds by Ion Trajectory Simulations

Xiaoyu Zhou,<sup>1</sup> Xinwei Liu,<sup>1</sup> Wenbo Cao,<sup>1</sup> Xiao Wang,<sup>2</sup> Ming Li,<sup>1</sup> Haoxue Qiao,<sup>3</sup>  
Zheng Ouyang<sup>1,2</sup>

<sup>1</sup>State Key Laboratory of Precision Measurement Technology and Instruments, Department of Precision Instrument, Tsinghua University, Beijing, 100084, China

<sup>2</sup>Weldon School of Biomedical Engineering, Purdue University, West Lafayette, IN 47907, USA

<sup>3</sup>Department of Physics, Wuhan University, Wuhan, 430072, China



**Abstract.** Gaussian distribution has been utilized to describe the global number density distribution of ion cloud in the Paul trap, which is known as the thermal equilibrium theory and widely used in theoretical modeling of ion clouds in the ion traps. Using ion trajectory simulations, however, the ion clouds can now also be treated as a dynamic ion flow field and the location-dependent features could now be characterized. This study was carried out to better understand the in-trap ion cloud properties, such as the local particle velocity and temperature. The local ion number densities were found to be heterogeneously distributed in terms of mean and distribution width; the velocity and temperature of the ion flow varied with pressure depending on the flow type of the neutral molecules; and the “quasi-static” equilibrium status can only be achieved after a certain number of collisions, for which the time period is pressure-dependent. This work provides new insights of the ion clouds that are globally stable but subjected to local *rf* heating and collisional cooling.

**Keywords:** Ion trajectory simulation, Gas field, Ion cloud, Local ion distribution

Received: 13 August 2017/Revised: 29 August 2017/Accepted: 7 September 2017/Published Online: 17 October 2017

## Introduction

Ions in the ion trap are subjected to two competitive effects: the acceleration in the radio-frequency (*rf*) electric field, known as *rf* heating, and the deceleration through the collisions with background molecules, known as buffer-gas cooling (Figure 1). This phenomenon was first studied by Dehmelt 49 years ago using the pseudopotential approximation [1], which described the *rf* trapping potential with an effective direct-current (DC) potential. Historically, the approximation greatly simplified the complicated multi-particle system, which otherwise could not be solved analytically. It also led to an important conclusion or assumption, known as the thermal equilibrium theory, that the equilibrium of ion cloud could be achieved through a large number of collisions with background molecules; and at the equilibrium the distributions of the ion cloud in the coordinate and velocity (or phase) space are Gaussian [2, 3]. The

theory has then been widely used to study the group behavior of the ion cloud [4–6], which is helpful for understanding the dynamic processes of ion transfer, ion trapping, ion activation, and ion ejection, providing guidance on precise control of the ions and shedding light on the design and optimization of the ion traps [7–10].

As a compromise to reach simplicity, two important features of ion trap were neglected in the pseudopotential approximation, viz., time-dependent dynamics of the *rf* field and dynamic gas field, which practically could have large impacts on ion cloud during ion transfer, ion storage, and mass analysis [11, 12]. The inaccuracy attributable to the approximation might have important impact on the understanding of the ion trap performance and implementation of ion processing [13, 14]. The thermal equilibrium theory sketches a frame but does not describe the details related to the local properties of the ion cloud, which could be important for understanding the dynamic processes of energy relaxation and energy exchange of the ions [15, 16]. For instance, local ion temperature is an important physiochemical parameter, determining the partitioning of ion energy from translational to vibrational (T to V) component

during ion activations and ion reactions [17, 18], as well as the conformational changes of biomolecules [19, 20].

Using ion trajectory simulations, such as those done with SIMION [21–23], ITSIM [23–26], ISIS [23, 27], electrohydrodynamic simulation (EHS) [28], and some other home written simulation programs [29–32], the local properties of the ion clouds in the ion traps can be accurately characterized. In this study, the EHS method was employed for performing simulations. The EHS method was originally developed for simulations with dynamic gas field [28]. In this study, as a first step toward the study of the local properties of the ion clouds, static gas fields were used. The ion cloud was analyzed in a view of field rather than a group of individual ions. The flow properties of the ion cloud, such as the varying velocities and temperatures at different locations of the ion trap, could be characterized.

## Method

A linear ion trap (LIT) was used as a model system for the study, with a field radius  $r_0$  of 3 mm, a length of 100 mm, and operated with a dipolar  $rf$  of 300  $V_{0-p}$  at a frequency of 1 MHz. The quadrupole field was established for trapping ions in the radial ( $x$  and  $y$ ) directions (Figure 1). The ion motions in the  $x$  and  $y$  directions were identical, except for a reversed phase. In the  $z$  direction, a weak DC field of 5 V was used for ion trapping. Because of the low penetration depth of the DC field, ion motion in the  $z$  direction around the trap center was almost free of electric fields, as a distinct comparison with the  $x$  and  $y$  directions. Static gas flow fields at two flow regimes, viz., viscous flow of 1 Torr and molecular flow of 7 mTorr, were employed for providing collisional cooling of the ions at different pressures.

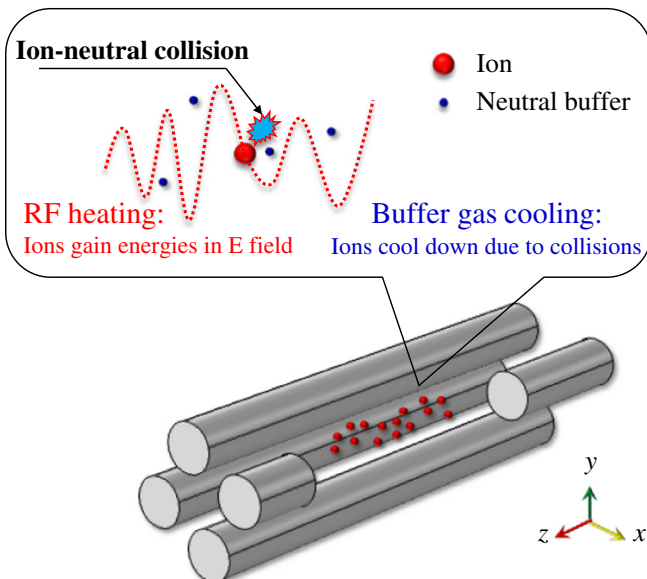


**Figure 1.** Schematic plot showing the ions subjected to the effects of  $rf$  heating and buffer-gas cooling in a linear Paul trap

The ion motion in the LIT was simulated by using the electrohydrodynamic simulation (EHS) program [28], which was developed and validated in our previous studies [33, 34]. Briefly, EHS calculates the ion trajectory through two successive processes in each step: first, the ion moves along a collision-free path and its motion is guided by the  $rf$  field in the LIT; and then, a collision modifies the ion velocity. The stochastic Monte-Carlo hard-sphere model was used for modeling the ion-neutral collisions in the simulations. The simulation was terminated after a time period long enough for reaching ion thermal equilibrium.

The simulation space was divided into grids, so that the local properties of the ion cloud could be sampled from the simulated ions fallen in each local grid point. Note that around the trap center, ion motion in the  $z$  direction is field free, and the local properties of the ion cloud along the  $z$  direction was assumed to be homogenous. Hence, only the  $x$ - $y$  plane of the LIT was divided into square grids for the study of the local ion properties, with grid size of 0.005–0.01  $r_0$ . Simulated ions within each grid were counted separately, allowing the extraction of local properties of the ion cloud [35], such as the bulk velocity  $\bar{v}$  and the temperature  $T$ :

$$\bar{v}_i(x_0, y_0) = \frac{1}{N_L} \sum_{n=1}^{N_L} v_i^n(x_0, y_0) \quad (1)$$

$$T_i(x_0, y_0) = \frac{m_{ion}}{N_L k_b} \sum_{n=1}^{N_L} \left[ v_i^n(x_0, y_0) - \bar{v}_i(x_0, y_0) \right]^2 \quad (2)$$

where  $v_i^n$  is the velocity component in the  $i$  direction of the  $n^{\text{th}}$  ion among the  $N_L$  ions within a local grid  $L(x_0, y_0)$ , and  $i$  denotes one of three normal directions,  $x$ ,  $y$ , or  $z$ .  $m_{ion}$  is the mass of the ions.  $K_b$  is the Boltzmann constant. The flow speed  $\bar{v}$  and scalar temperature  $T$  of the ion cloud at local  $L$  are also defined as the magnitude of the velocity  $\bar{v}$  and the average of three normal components of the temperature  $T$ , respectively:

$$\bar{v} = \sqrt{\bar{v}_x^2 + \bar{v}_y^2 + \bar{v}_z^2} \quad (3)$$

$$T = \frac{1}{3} (T_x + T_y + T_z) \quad (4)$$

The method development for the extraction of local properties of the ion cloud, viz., ion velocities and temperatures, was motivated by the method used in direct simulation Monte-Carlo (DSMC) method [35], in which a large number of simulated gas molecules are used to mimic real gas flows, and the local properties of the gas flow field were extracted based on the statistics of local gas molecules. For both DSMC and the method used here, the quality of the simulated local properties depends on the number of simulated particles. In this work, at

least  $10^5$  simulated ions were used to ensure the fluctuation of the local properties of the ion cloud were, typically, better than 15%. Space charge effect was not considered in the simulations to reduce the computational burden.

## Results and Discussion

Protonated imatinib ions of  $m/z$  494, with Gaussian distributions of initial position and velocity, were placed in the LIT at a temperature of 300 K and a pressure of 1 Torr. It was found that after cooling in air buffer for 0.3 ms, the number density  $n$  of all the imatinib ions in the trap (global  $n$ , red circle in Figure 2a), can be stable with Gaussian distributions in coordinate (Figure 2a) and velocity (red curve, Figure 2b) space, which matched well with the classic thermal equilibrium theory. However, because of inverted  $rf$  phase, the distribution widths  $\sigma_x$  and  $\sigma_y$  of the ions in the  $x$  and  $y$  directions of coordinate space, respectively, were different, about 0.06 and 0.04  $r_0$  (Figure 2a). The result indicated that even at high pressure of 1 Torr, the motion phase of the ions attributable to the  $rf$  phase would not be averaged by frequent ion-neutral collisions, resulting in a fluctuation of about 50% in the shape of ion cloud at “thermal equilibrium” status. The result indicates that the  $rf$  phase could have a relatively large impact on manipulation of the ion cloud, shaping the ion clouds during emittance or acceptance by the quadrupole devices [36], such as quadrupole ion traps, quadrupole ion guides, and quadrupole mass filters.

Further investigation of the ion cloud distribution indicated that the local ion distributions (local  $n$ ) in the velocity space were different from the global  $n$  and were heterogeneously distributed (Figure 2b). The local  $n$  at four different local points, L1 ( $x = -0.03 r_0$ , black curve), L2 ( $x = 0.015 r_0$ , orange curve), L3 ( $x = 0.03 r_0$ , blue curve), and L4 ( $x = 0.04 r_0$ , green curve) had obvious deviation from the global  $n$  (red curve), in terms of the means and standard deviations (SDs) shown in Figure 2c. From Figure 2c, it can be found that the fluctuations of the means and SDs were within 15% of the simulated values,

indicating that the simulation quality was good enough to study the change of ion properties at different locations of the ion trap. Physically, the mean and standard deviation (SD) of the ion population  $n$  correspond to the bulk speed  $\bar{v}$  and temperature  $T$  of the ions (Equations 1 and 2). Using the method in this study, the ion local heterogeneous distributions could be individually characterized; however, it should be noted that the heterogeneous distribution of ion local distributions cannot be observed globally because of the mutual counteraction of local distortions (see L1 and L3 as an example).

Pressures at about 1 Torr were shown to be of a high pressure range where mass analysis could still be effectively performed [8, 37–39]. The ion-neutral collision rate at this pressure is ca.  $10^7 \text{ s}^{-1}$ . Generally it is believed that electric field at higher pressures is much less effective on manipulation of the ion beam or cloud [40]. Our finding shown in Figure 2 indicates that the electric field can be effective in steering the ions at 1 Torr, in terms of the time-dependent motion phase and spatially related field strength. The steering effect by electric field would be even more significant at lower pressures such as 7 mTorr, at which collision induced dissociation is typically performed [41].

With the ion distribution locally characterized, detailed flow properties of the ion cloud, such as the flow velocity  $\bar{v}$  and temperature  $T$  [35], could then be extracted. It was found that motion behavior of the ion cloud was dependent on the continuity of the neutral gas flow. For example, in the relatively more viscous flow regime at pressure 1 Torr (Figure 3a–d), most of the ions were compacted within a region under the low field limit of  $10 \text{ Vcm}^{-1}\text{Torr}^{-1}$  [42]. The frequent ion-neutral collisions gave rise to a drift motion  $\bar{v}$  of the ions in the electric field (Figure 3a). The asymmetry of  $\bar{v}$  in the  $x$  and  $y$  directions was attributable to the inverted  $rf$  phase between the two directions. Close-up plot of  $\bar{v}$  in its three normal components along the positive  $x$  axis is shown in Figure 3b. It was found that  $\bar{v}_x$  increased linearly with local electric field strength,  $E_x$ , (black curve), similar to that found in the ion mobility experiments, i.e.,  $\bar{v}_x = KE_x$ , where  $K$  is the ion mobility coefficient. The low  $\bar{v}_y$  and  $\bar{v}_z$  (red and blue curves, respectively) were

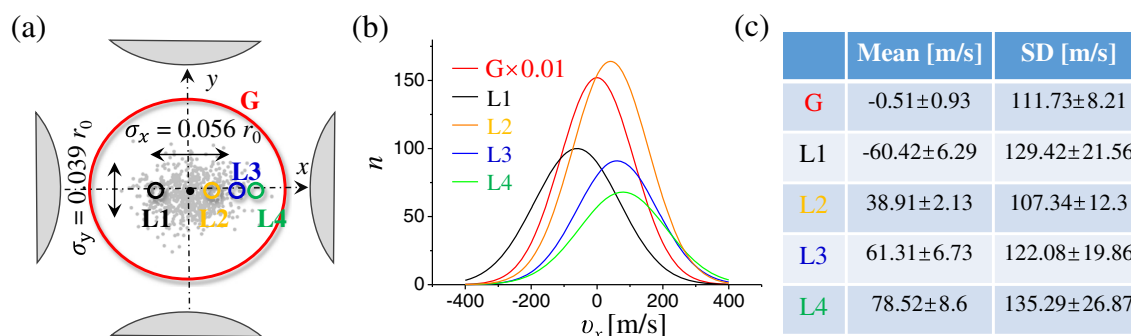


**Figure 2.** (a) Protonated imatinib ions,  $m/z$  494, in the LIT at thermal equilibrium. The ion cloud is not shown to scale. (b) Number density distributions of all the ions (global  $n$ , red curve) and the local ions (local  $n$ ) at points L1 ( $x = -0.03 r_0$ , black curve), L2 ( $x = 0.015 r_0$ , orange curve), L3 ( $x = 0.03 r_0$ , blue curve), and L4 ( $x = 0.04 r_0$ , green curve) in the  $v_x$  space. The intensity of the global ions is rescaled by a factor of 0.01. (c) The means and standard deviations (SDs) of the global and local ion distributions, which were obtained from three replicates

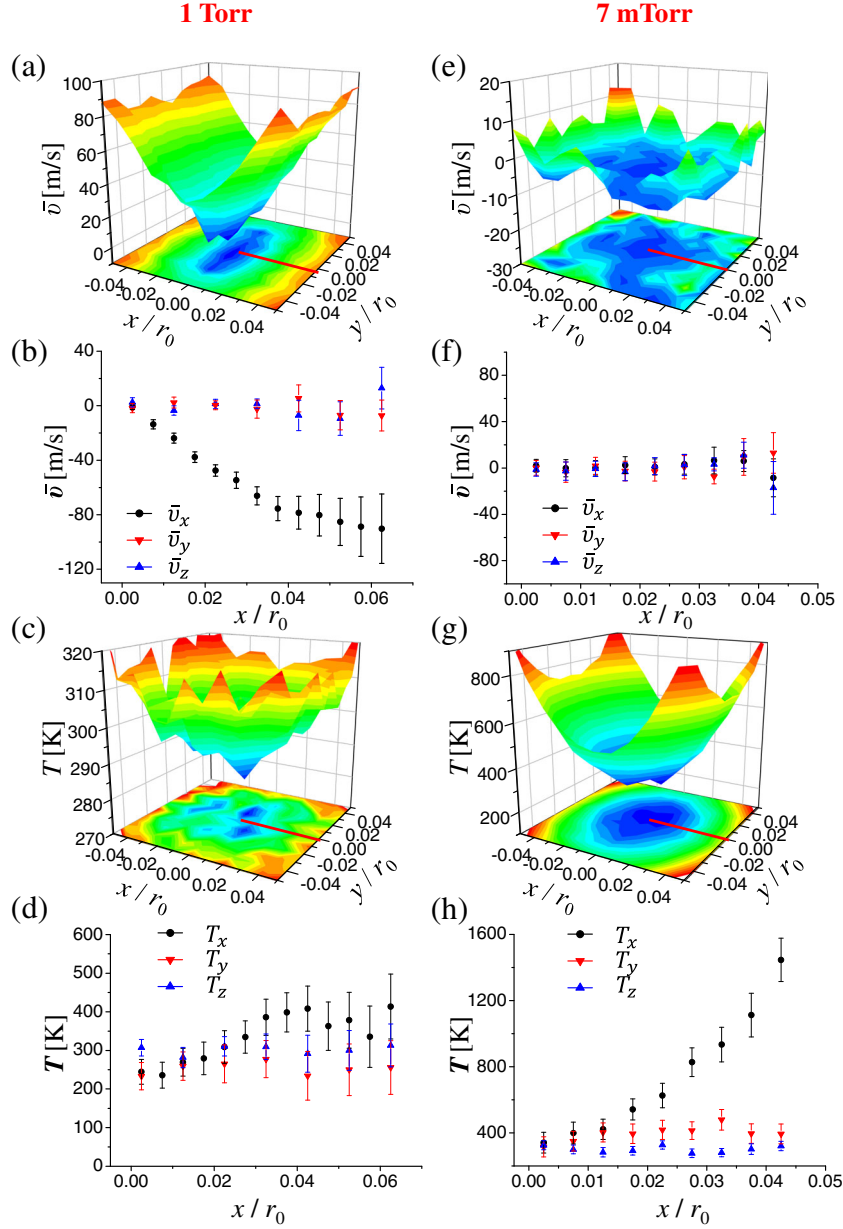


**Figure 3.** Contour plot of the flow speed,  $\bar{v}$ , of the ion cloud at 1 Torr (a) and 7 mTorr (e). Flow velocity vector,  $\bar{v}$ , of the ion cloud along the positive  $x$  coordinate at 1 Torr (b) and 7 mTorr (f), marked as red lines in (a) and (e), accordingly, in the three normal directions,  $x$  (black curve),  $y$  (red curve), and  $z$  (blue curve). Contour plot of the scalar temperature,  $T$ , of the ion cloud at 1 Torr (c) and 7 mTorr (g). Flow temperature vector,  $T$ , of the ion cloud along the positive  $x$  coordinate at 1 Torr (d) and 7 mTorr (h), marked as red lines in (c) and (g), accordingly, in the three normal directions,  $x$  (black curve),  $y$  (red curve), and  $z$  (blue curve). The  $\bar{v}$  and  $T$  at 1 Torr and 7 Torr are obtained from the same  $rf$  phase with three replicates

results of the lack of  $E_y$  and  $E_z$  field components. At this pressure, the ion temperature  $T$  was about 300 K, not with significant changes but small fluctuations (Figure 3c). Close-up plot of  $T$  in its three normal components indicated that  $T_x$  increased slightly due to the heating of the  $rf$  field (black curve), while  $T_y$  and  $T_z$  whereas unaffected (red and blue curves, respectively).

As a comparison, the  $\bar{v}$  and  $T$  in the molecular flow regime are shown in Figure 3e–h. The ion cloud at 7 mTorr was not shown to have an obvious directed flow, viz.  $\bar{v} \approx 0$  (Figure 3e, f);

however, significant heating of the ion cloud was observed (Figure 3g). Close-up plots of  $T$  in its three normal components showed that  $T_x$  increased linearly to the square of the  $E_x$  (black curve of Figure 3h). The observation determined that the temperature of the ion cloud at thermal equilibrium are location-dependent in the trap and can be 3-fold higher than the room temperature at one  $\sigma_x$ ,  $x = 0.03 r_0$ . This is different from the knowledge based on conventional treatment [4–6], which assumes a uniform distribution for the ion cloud at thermal equilibrium under room temperature. The variation of the ion

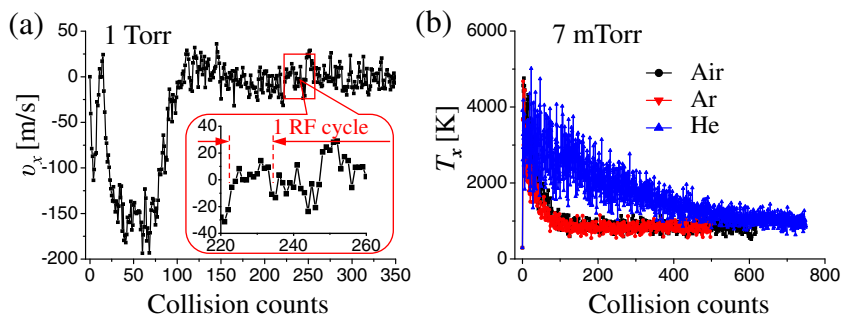


**Figure 4.** (a) Local flow velocity in the  $x$  direction,  $\bar{v}_x$ , of the ion cloud at grid L1 in Figure 2a as a function of the collision counts at pressure 1 Torr. (b) Local ion temperature in the  $x$  direction,  $T_x$ , of the ion cloud at L1 as a function of the collision counts at pressure 7 mTorr with air (black curve), Ar (red curve), and He (blue curve) as buffer gases. Close-up of (a) between collision counts, 220 and 260, is shown in the inset

temperature within the trap implies that the collision induced fragmentation (CID) efficiency is location-dependent. CID processes are more likely to gain energy at higher temperature (or fringe) regions and relax at lower temperature (or central) regions of the trap, which is certainly related to the slow heating mechanism for ion activations for CID or ion reactions within the trap [15, 18].

By comparing the two cases, it is obvious that the heating effect of the  $rf$  field depends on the type of gas flow in which the ion cloud immersed. For viscous flows,  $rf$  heating gives rise to the drift motion of the ion cloud, corresponding to directed translational energy; but for molecular flows, it contributes to the stochastic translational energy of the ion cloud, leading to an increase of ion temperature or internal energy. Here, it is obvious that pressure plays an important role in modifying the local bulk velocity and temperature of the ion cloud. Our finding supports experimental observations that the pressures of 1 Torr is suitable for performing ion mobility separation [43], whereas 7 mTorr is more suitable for ion activation [41].

The transition process of the ion cloud from the initial state to the final thermal equilibrium state was also characterized. The ion cloud drift velocity  $\bar{v}$  has significant changes at 1 Torr (Figure 3a). The  $\bar{v}_x$  at grid L1 (Figure 2a) was recorded as a function of the collision counts  $\tau = \lambda/v_{rel}$  for monitoring the process (Figure 4a), where  $\lambda$  is the mean free path of the ions, and the  $v_{rel}$  is the mean of the relative speed between the ion and neutral molecule. It has been shown in Figures 2 and 3 that the actual equilibrium distributions of the local ions were not uniformly of a single Gaussian, but with different means and SDs and should be location-dependent. Assuming a group of ions entered or were produced inside the trap, with uniform initial means of zero and SDs of 300 K for the Gaussian distribution at each location inside an ion trap, the  $\bar{v}_x$  at L1 would have a sudden change within the first 100 ion-neutral collisions, and then gradually reach a location-dependent equilibrium (Figure 4a). The sudden change of ion velocity can be attributed to the ion-neutral collisions with high probability, which guide the ion cloud at each location to change from the non-equilibrium to equilibrium distribution with location-dependent means and SDs. It requires at least a time

corresponding to 100 ion-neutral collisions, ca. 15  $\mu$ s at 1 Torr, for the ion cloud to thermalize locally. Even at such a high pressure, the effect due to the  $rf$  phase cannot be averaged out by the collisions; thus, relatively large fluctuations of  $\bar{v}_x$  are observed within an  $rf$  cycle (inset of Figure 4a).

The fluctuation should be much more significant at 7 mTorr because of a lower frequency of ion-neutral collisions. For pressure at 7 mTorr,  $T$  has a much more significant change than  $\bar{v}$  (Figure 3), and thus is used as an index for modeling the dynamic equilibrium process (Figure 4b). The  $T$  has been averaged by a  $rf$  cycle. A trend similar to that at 1 Torr was observed, indicating that even at lower pressures, thermal equilibrium could be achieved after averaging the  $rf$  phase effect. The use of different buffers, including air (molecular weight, MW=29, black curve), Ar (MW=40, red curve), and He (MW=4, blue curve) does not change the properties of the ion cloud at equilibrium, such as the  $T_x$ ; however, they changed significantly the dynamics of the process toward the thermal equilibrium state. For example, the ion temperature ramps rapidly from 300 K to above 4000 K in the first few collisions, and then the ion cloud reaches equilibrium through 100 collisions (ca. 2 ms) in air and Ar, but the time is elongated to 700 collisions (ca. 15 ms) for He.

## Conclusion

As a summary, using the electro-hydrodynamic simulation method, the local properties of the ion cloud were studied. The ion number density distribution of the ion cloud at stable status (as conventionally called thermal equilibrium) in the ion trap is location-dependent, rather than a globally uniform Gaussian. The heterogeneity of the distribution, in terms of the mean and SD, originate from the effect by dynamic electric field, viz.  $rf$  heating. In a viscous flow regime, e.g., at a pressure of 1 Torr, the ion cloud gains energy from the  $rf$  heating, which is subsequently transformed into a directed drift motion. However, in a molecular flow regime, e.g., at 7 mTorr, the energy is transformed into stochastic ion motions. At a stable status for viscous flow regime, the motion phase of the ion cloud

attributable to the *rf* persists, frequently even with highly ion-neutral collisions. For molecular flow regime, the stable status could be reached but takes a significantly longer period of time.

The implication from the results in this work and onto future simulation studies could be intriguing. The potential errors due to the wrongfully assigned local initial conditions could be removed eventually, after a certain number of ion-neutral collisions when a location-dependent balance is reached with collisional cooling and *rf* heating. However, the time period required is pressure-dependent and could be as long as 150 ms at  $1 \times 10^{-4}$  Torr. The actual impact on the accuracy of the simulation is expected to be case by case; however, this should be a factor to be included in the consideration for the simulation work.

Treating the ion cloud as a field rather than counting individual ions would facilitate the characterization of ion cloud involving a large number of ions, which is subjected to other factors such as the pressure. The space charge effect was not considered in the simulation. Its impact on the local properties of the ions is expected to be broadening the SD but not changing the mean of the velocity distribution.

## Acknowledgments

The work was supported by National Natural Science Foundation of China (grant 21627807).

## References

- Dehmelt, H.G.: Radiofrequency spectroscopy of stored ions, i: storage. *Adv. At. Mol. Phys.* **3**, 53–72 (1968)
- March, R.E., Todd, J.F.J.: Radio frequency quadrupole technology: evolution and contributions to mass spectrometry. *Int. J. Mass Spectrom.* **377**, 316–328 (2015)
- March, R.E.: An introduction to quadrupole ion trap mass spectrometry. *J. Mass Spectrom.* **32**, 351–369 (1997)
- Guan, S., Marshall, A.G.: Equilibrium space charge distribution in a quadrupole ion trap. *J. Am. Soc. Mass Spectrom.* **5**, 64–71 (1994)
- Li, G.-Z., Guan, S., Marshall, A.G.: Comparison of equilibrium ion density distribution and trapping force in penning, paul, and combined ion traps. *J. Am. Soc. Mass Spectrom.* **9**, 473–481 (1998)
- Guo, D., Wang, Y., Xiong, X., Zhang, H., Zhang, X., Yuan, T., Fang, X., Xu, W.: Space charge induced nonlinear effects in quadrupole ion traps. *J. Am. Soc. Mass Spectrom.* **25**, 498–508 (2014)
- Lammert, S.A., Plass, W.R., Thompson, C.V., Wise, M.B.: Design, optimization and initial performance of a toroidal rf ion trap mass spectrometer. *Int. J. Mass Spectrom.* **212**, 25–40 (2001)
- Xu, W., Song, Q., Smith, S.A., Chappell, W.J., Ouyang, Z.: Ion trap mass analysis at high pressure: a theoretical view. *J. Am. Soc. Mass Spectrom.* **20**, 2144–2153 (2009)
- Remes, P.M., Syka, J.E.P., Kovtoun, V.V., Schwartz, J.C.: Insight into the resonance ejection process during mass analysis through simulations for improved linear quadrupole ion trap mass spectrometer performance. *Int. J. Mass Spectrom.* **370**, 44–57 (2014)
- Dawson, P.H.: Quadrupole mass analyzers: performance, design, and some recent applications. *Mass Spectrom. Rev.* **5**, 1–37 (1986)
- Cox, K.A., Cleven, C.D., Cooks, R.G.: Mass shifts and local space charge effects observed in the quadrupole ion trap at higher resolution. *Int. J. Mass Spectrom. Ion Process.* **144**, 47–65 (1995)
- Snyder, D.T., Peng, W.-P., Cooks, R.G.: Resonance methods in quadrupole ion traps. *Chem. Phys. Lett.* **668**, 69–89 (2017)
- Gross, M.L.: High performance mass spectrometry. *Anal. Chem.* **50**, 530A–530A (1978)
- Xian, F., Hendrickson, C.L., Marshall, A.G.: High resolution mass spectrometry. *Anal. Chem.* **84**, 708–719 (2012)
- Majumdar, T.K., Clairet, F., Tabet, J.C., Cooks, R.G.: Epimer distinction and structural effects on gas-phase acidities of alcohols measured using the kinetic method. *J. Am. Chem. Soc.* **114**, 2897–2903 (1992)
- Wunderlich, C., Morigi, G., Reiß, D.: Simultaneous cooling of axial vibrational modes in a linear ion trap. *Phys. Rev. A.* **72**, 023421 (2005)
- Basic, C., Eyler, J.R., Yost, R.A.: Probing trapped ion energies via ion-molecule reaction kinetics: quadrupole ion trap mass spectrometry. *J. Am. Soc. Mass Spectrom.* **3**, 716–726 (1992)
- McGee, W.M., McLuckey, S.A.: Efficient and directed peptide bond formation in the gas phase via ion/ion reactions. *Proc. Natl. Acad. Sci. U. S. A.* **111**, 1288–1292 (2014)
- Ruotolo, B.T., Hyung, S.-J., Robinson, P.M., Giles, K., Bateman, R.H., Robinson, C.V.: Ion mobility-mass spectrometry reveals long-lived, unfolded intermediates in the dissociation of protein complexes. *Angew. Chem. Int. Ed.* **46**, 8001–8004 (2007)
- Hopper, J.T.S., Oldham, N.J.: Collision induced unfolding of protein ions in the gas phase studied by ion mobility-mass spectrometry: the effect of ligand binding on conformational stability. *J. Am. Soc. Mass Spectrom.* **20**, 1851–1858 (2009)
- Quarmby, S.T., Yost, R.A.: Fundamental studies of ion injection and trapping of electrosprayed ions on a quadrupole ion trap. *Int. J. Mass Spectrom.* **190/191**, 81–102 (1999)
- Lynn, E.C., Chung, M.-C., Han, C.-C.: Characterizing the transmission properties of an ion funnel. *Rapid Commun. Mass Spectrom.* **14**, 2129–2134 (2000)
- Forbes, M.W., Sharifi, M., Croley, T., Lausevic, Z., March, R.E.: Simulation of ion trajectories in a quadrupole ion trap: a comparison of three simulation programs. *J. Mass Spectrom.* **34**, 1219–1239 (1999)
- Bui, H.A., Graham Cooks, R.: Windows version of the ion trap simulation program ITSIM: a powerful heuristic and predictive tool in ion trap mass spectrometry. *J. Mass Spectrom.* **33**, 297–304 (1998)
- Plass, W.R., Cooks, R.G.: A model for energy transfer in inelastic molecular collisions applicable at steady state or non-steady state and for an arbitrary distribution of collision energies. *J. Am. Soc. Mass Spectrom.* **14**, 1348–1359 (2003)
- Wu, G., Cooks, R.G., Ouyang, Z., Yu, M., Chappell, W.J., Plass, W.R.: Ion trajectory simulation for electrode configurations with arbitrary geometries. *J. Am. Soc. Mass Spectrom.* **17**, 1216–1228 (2006)
- Londry, F.A., Alfred, R.L., March, R.E.: Computer simulation of single-ion trajectories in paul-type ion traps. *J. Am. Soc. Mass Spectrom.* **4**, 687–705 (1993)
- Zhou, X., Ouyang, Z.: Flowing gas in mass spectrometer: method for characterization and impact on ion processing. *Analyst.* **139**, 5215–5222 (2014)
- Douglas, D.J., French, J.B.: Collisional focusing effects in radio frequency quadrupoles. *J. Am. Soc. Mass Spectrom.* **3**, 398–408 (1992)
- Julian, R.K., Nappi, M., Weil, C., Cooks, R.G.: Multiparticle simulation of ion motion in the ion trap mass spectrometer: resonant and direct current pulse excitation. *J. Am. Soc. Mass Spectrom.* **6**, 57–70 (1995)
- Zhang, Z., Quist, H., Peng, Y., Hansen, B.J., Wang, J., Hawkins, A.R., Austin, D.E.: Effects of higher-order multipoles on the performance of a two-plate quadrupole ion trap mass analyzer. *Int. J. Mass Spectrom.* **299**, 151–157 (2011)
- Xiong, X., Xu, W., Fang, X., Deng, Y., Ouyang, Z.: Accelerated simulation study of space charge effects in quadrupole ion traps using gpu techniques. *J. Am. Soc. Mass Spectrom.* **23**, 1799–1807 (2012)
- Zhou, X., Ouyang, Z.: Following the ions through a mass spectrometer with atmospheric pressure interface: simulation of complete ion trajectories from ion source to mass analyzer. *Anal. Chem.* **88**, 7033–7040 (2016)
- Zhou, X., Ouyang, Z.: Ion transfer between ion source and mass spectrometer inlet: electro-hydrodynamic simulation and experimental validation. *Rapid Commun. Mass Spectrom.* **30**, 29–33 (2016)
- Bird, G.A.: *Molecular gas dynamics and the direct simulation of gas flows.* Oxford University Press, New York (1994)
- Jyothi, S., Ray, T., Rangwala, S.A.: Phase-sensitive radial extraction and mass spectrometry of trapped ions in a compact geometry. *Appl. Phys. B Lasers Opt.* **118**, 131–138 (2015)
- Blakeman, K.H., Wolfe, D.W., Cavanaugh, C.A., Ramsey, J.M.: High pressure mass spectrometry: the generation of mass spectra at operating pressures exceeding 1 Torr in a microscale cylindrical ion trap. *Anal. Chem.* **88**, 5378–5384 (2016)

38. Xu, W., Maas, J.B., Boudreau, F.J., Chappell, W.J., Ouyang, Z.: Nondestructive ion trap mass analysis at high pressure. *Anal. Chem.* **83**, 685–689 (2011)
39. Song, Q., Xu, W., Smith, S.A., Gao, L., Chappell, W.J., Cooks, R.G., Ouyang, Z.: Ion trap mass analysis at high pressure: an experimental characterization. *J. Mass Spectrom.* **45**, 26–34 (2010)
40. Kelly, R.T., Tolmachev, A.V., Page, J.S., Tang, K., Smith, R.D.: The ion funnel: theory, implementations, and applications. *Mass Spectrom. Rev.* **29**, 294–312 (2010)
41. McLafferty, F.: Tandem mass spectrometry. *Science.* **214**, 280–287 (1981)
42. Hernandez, D.R., DeBord, J.D., Ridgeway, M.E., Kaplan, D.A., Park, M.A., Fernandez-Lima, F.: Ion dynamics in a trapped ion mobility spectrometer. *Analyst.* **139**, 1913–1921 (2014)
43. Kanu, A.B., Dwivedi, P., Tam, M., Matz, L., Hill, H.H.: Ion mobility-mass spectrometry. *J. Mass Spectrom.* **43**, 1–22 (2008)